ARTICLE COVERSHEET

LWW_CONDENSED(7.75X10.75)

SERVER-BASED

Article : JCAT_220300
Creator : apps_lww
Date : Thursday December 29th 2022
Time : 05:11:14
Number of Pages (including this page) : 9

Effect of 320-Row Computed Tomography Acquisition Technology on Coronary Computed Tomography Angiography–Derived Fractional Flow Reserve Based on Machine Learning: Systolic and Diastolic Scan Acquisition

AQ1 *Fengfeng Yang,* Ke Shi,† Yuhuan Chen,‡ Youbing Yin,‡ Yang Zhao,* and Tong Zhang†*

Background: The aim of the study is to investigate the performance of coronary computed tomography angiography (CCTA)–derived fractional flow reserve (CT-FFR) in the same patient evaluated by different systolic and diastolic scans, aiming to explore whether 320-slice CT scanning acquisition protocol has an impact on CT-FFR value.

Methods: One hundred forty-six patients with suspected coronary artery stenosis who underwent CCTA examination were included into the study. The prospective electrocardiogram gated trigger sequence scan was performed and electrocardiogram editors selected 2 optimal phases of systolic phase (preset collection trigger at 25% of R-R interval) and diastolic phase (preset collection trigger at 75% of R-R interval) for reconstruction. The lowest CT-FFR value (the CT-FFR value at the distal end of each vessel) and the lesion CT-FFR value (at 2 cm distal to the stenosis) after coronary artery stenosis were calculated for each vessel. The difference of CT-FFR values between the 2 scanning techniques was compared using paired Wilcoxon signed-rank test. Pearson correlation value and Bland-Altman were performed to evaluate the consistency of CT-FFR values.

Results: A total of 366 coronary arteries from the remaining 122 patients were analyzed. There was no significant difference regarding the lowest CT-FFR values between systole phase and diastole phase across all vessels. In addition, there was no significant difference in the lesion CT-FFR value after coronary artery stenosis between systole phase and diastole phase across all vessels. The CT-FFR value between the 2 reconstruction techniques had excellent correlation and minimal bias in all groups. The correlation coefficient of the lesion CT-FFR values for left anterior descending branch, left circumflex branch, and right coronary artery were 0.86, 0.84, and 0.76, respectively.

Conclusions: Coronary computed tomography angiography–derived fractional flow reserve based on artificial intelligence deep learning neural network has stable performance, is not affected by the acquisition phase technology of 320-slice CT scan, and has high consistency with the evaluation of hemodynamics after coronary artery stenosis.

Key Words: computed tomography, coronary computed tomography angiography, computed tomography acquisition technology, fractional flow reserve, machine learning

(*J Comput Assist Tomogr* 2022;00: 00–00)

From the *Department of Radiology, The Second Hospital of Tianjin Medical University, Tianjin.; †Department of Radiology, The Fourth Affiliated Hospital, AQ2 Harbin Medical University, Harbin.; and ‡Keya Medical, Shenzhen, China.

Received for publication April 24, 2022; accepted September 22, 2022.

AQ3 Correspondence to: Tong Zhang, Department of Radiology, The Fourth Affiliated Hospital, Harbin Medical University, Harbin 150001, China (e-mail: zhangt0415@163.com).

The authors declare no conflict of interest.

F.Y. and K.S. contributed equally to this work.

F.Y. and T.Z. conceived and designed the experiments. KS performed the experiments. F.Y. and Y.Z. analyzed the data. Y.Z., Y.C., and Y.Y. contributed reagents/materials/analysis tools. F.Y. and T.Z. wrote and submitted the manuscript. All authors read and approved the final version of the manuscript.

DOI: 10.1097/RCT.0000000000001423

Coronary computed tomography angiography (CCTA)–derived fractional flow reserve (CT-FFR) is a new technology that combines computer imaging reconstruction and functional analysis of fluid dynamics simulation.[1–3] In recent years, many studies have reported that CT-FFR has a higher diagnostic accuracy than other noninvasive examination modalities for heart disease, when compared with the criterion standard invasive FFR.[2,4–6] Coronary computed tomography angiography–derived fractional flow reserve has emerged as a promising noninvasive test to assess hemodynamic severity of coronary artery disease (CAD).[7]

Ideally, a complete data set of the entire cardiac anatomy should be obtained within monophasic cardiac cycles with the patient remaining still.[8] However, it is not possible to obtain the image of many patients' heartbeat at the same time because of uncontrollable rapid heart rate and the limitations of the scanning equipment.[9,10] These continuous heartbeat images need to be stitched together during postprocessing; hence, the different segments of the artery from proximal to distal direction lack the time consistency of contrast agent turbidity.[9,11] Piecewise reconstruction techniques using reconstruction from 2 or more segments of a continuous cardiac cycle can improve time resolution, but this technique can produce fuzzy artifacts if the heart rate changes during the scan.[8] However, it is not clear whether the temporal heterogeneity of contrast agent delivery will affect the diagnostic performance of CT-FFR.

Therefore, this study retrospectively analyzed the performance of CT-FFR in the same patient evaluated by different systolic and diastolic scans, aiming to explore whether 320-slice CT scanning acquisition protocol has an impact on CT-FFR value.

MATERIALS AND METHODS

Patients

The study was conducted in accordance with the Declaration of Helsinki (as revised in 2013). From December 2020 to December 2021, a total of 146 patients with suspected coronary artery stenosis in clinic who underwent CCTA examination were included into the retrospective study. Patients with severe arrhythmia, severe artifacts, severe calcification, any coronary malformations (coronary fistula, abnormal coronary origin, abnormal coronary dilation), and a history of coronary stent or bypass surgery were excluded. This study was approved by the medical ethics committee of The Fourth Affiliated Hospital. All patients' informed consent for this retrospective study was waived. Figure 1 shows a detailed F1 time line of the study protocol.

Coronary CTA

Toshiba 320-row CT (Aquilion ONE; Toshiba, Tokyo, Japan) was used for data collection. For patients whose heart rate was greater than 80 per minute, 25- to 50-mg metoprolol was administrated orally, and scanning was performed after the heart rate was reduced

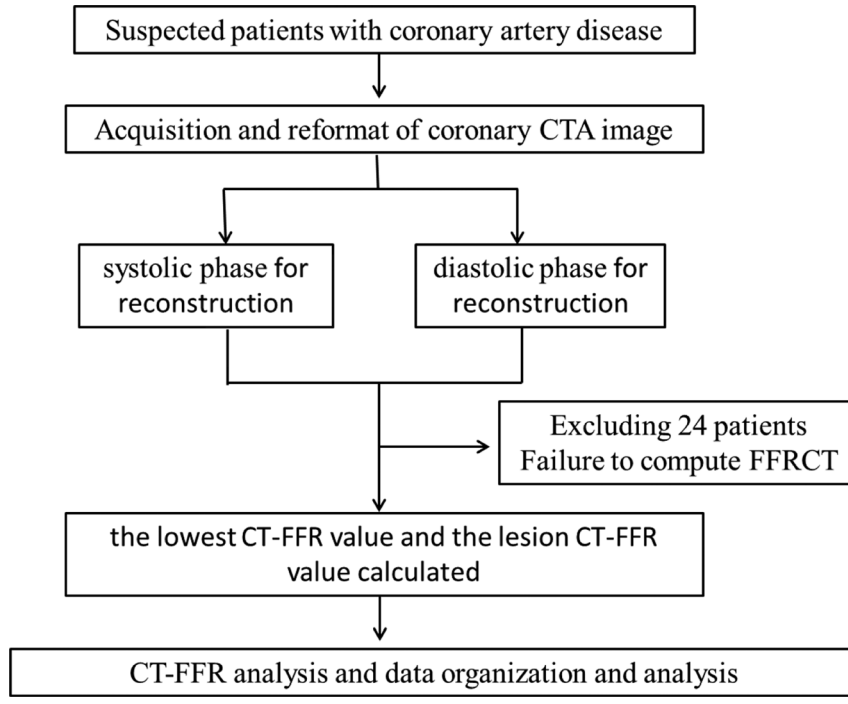

FIGURE 1. Strategy for CT-FFR analysis and data processing in this study. Twenty-four patients were excluded because their CCTA images were not available for CT-FFR computational analysis. Eleven patients were excluded because of severe coronary artery artifacts due to severe calcification, 3 patients had coronary artery malformation, and 10 patients had a history of coronary artery stenting.

less than 70 per minute. Indwelling 18G trocar was placed in the antecubital vein. The nonionic iodine contrast agent (350 mg/L) was injected into 40- to 70-mL nonionic iodine contrast agent at the flow rate of 6.0 mL/s using a double-channel high-pressure syringe. Three hundred twenty detector row CT images were acquired with 350-millisecond gantry rotation time and 120-kV tube voltage. Dose of contrast agent and the bulb current were selected based on body mass index. The radiation dose was 1.0 ± 0.5 mSv. Each patient was placed in the supine position and connected to the electrocardiogram (ECG) monitor, following which the ventricular layer monitoring scan was performed. The prospective ECG-gated trigger sequence scan was performed using contrast agent group injection tracking method, ranging from 1.0 cm below the tracheal carina to 1.5 cm at the lower edge of the heart. The ECG editors selected 2 optimal phases of systolic phase (preset collection trigger at 25% of R-R interval) and diastolic phase (preset collection trigger at 75% of R-R interval) for reconstruction, with a thickness of 0.5 mm and a spacing of 0.5 mm. The collected data were transferred to Vitrea FX workstation (Canon Medical, Japan) for postprocessing, including multiplanar reformat, curved multiplanar reformat, volume reformat, etc.

The image quality evaluation is divided into the following 4 grades: poor, medium, good, and excellent. Only images with good to excellent systolic and diastolic image quality were included in further analysis. All CT images were analyzed separately by 2 experienced senior radiologists. When there was a difference in the opinion, they arrived at a final conclusion after discussing it in detail. The coronary tree was assessed according to the 18-segment coronary artery segmentation system published by the American Society for Cardiovascular Computed Tomography in 2014, and the severity of stenosis at each segment was visually assessed and patients were classified according to the Coronary Artery Disease Reporting and Data System.[12] The evaluation of stenosis degree is divided into the following 6 grades: 0%, no visible stenosis; (1) minimal stenosis (stenosis degree 1%–24%); (2) mild stenosis (stenosis degree 25%–49%); (3) moderate stenosis (stenosis degree 50%–69%); (4) severe stenosis (70%–99% stenosis); and (5) occlusion (stenosis degree 100%).[13] Diameter stenosis ≥50% was defined as obvious obstructive coronary artery.

Coronary Computed Tomography Angiography–Derived Fractional Flow Reserve Analysis

An artificial intelligent deep learning–based software (DEEP VESSEL FFR; KEYA Medical, China), which was approved for clinical use by Chinese National Medical Products Administration, was used for the calculation of CT-FFR in this work. Previous studies have reported that the performance ranged from 87.3% to 90.4% using invasive FFR as reference.[14,15] Its application on the patient outcome has also been reported.[16] This deep learning algorithm calculates CT-FFR from the anatomical and imaging information from the complex coronary artery tree. It takes the centerline and images as inputs and calculates CT-FFR for the whole artery tree. The model fully considers the artery tree structure, lesion-specific information, spatial relationship, and the influences of other branches for the blood flow dynamics.[14,17]

All CCTA data are transmitted to the cloud workstation in standard Digital Imaging and Communications in Medicine format. Based on the training and learning of fluid dynamics simulation data of a large number of coronary cases, the software calculated and obtained the blood flow reserve fraction, and the output time was less than 10 minutes per case. The software provides a specific 3-dimensional model of the coronary arteries, allowing the investigator to obtain CT-FFR values along any given point in the length of the coronary vessels.

The lowest CT-FFR value (the CT-FFR value at the distal end of each vessel) was recorded for each vessel, and if the CT-FFR value was ≤0.8, the patient was classified as having obstructive CAD (Fig. 2). F2 Moreover, the lesion CT-FFR value (at 2 cm distal to the stenosis)

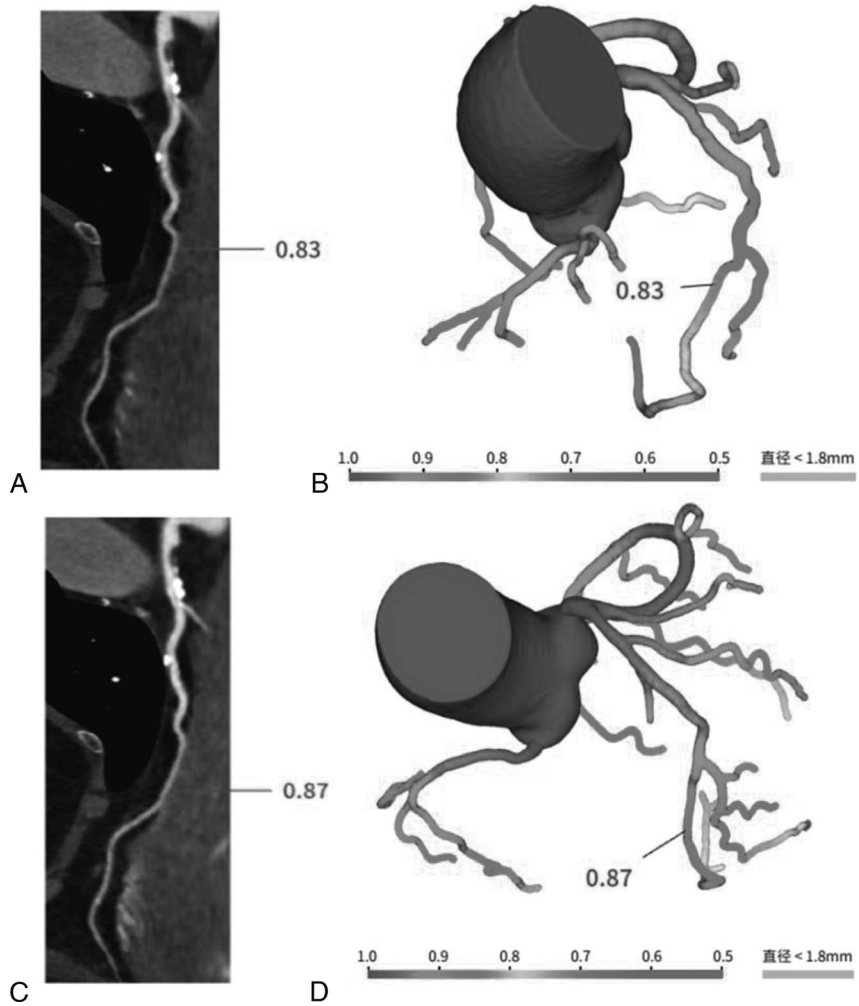

FIGURE 2. An example of the CCTA and the corresponding CT-FFR model, a 72-year-old female patient. A and C, LAD with moderate stenosis imaged by CCTA selected 2 optimal phases of systolic phase and diastolic phase for reconstruction. B, The corresponding CT-FFR model of systolic phase for reconstruction. The lesion CT-FFR value (at 2 cm distal to the lesion) after coronary artery stenosis was shown as 0.83. D, The corresponding CT-FFR model of diastolic phase for reconstruction. The lesion CT-FFR value (at 2 cm distal to the lesion) after coronary artery stenosis was shown as 0.87. Figure 2 can be viewed in color online at www.jcat.org.

after coronary artery stenosis was recorded using the same ischemia threshold corresponding to the location of coronary artery stenosis and corresponding 3D coronary artery model (Fig. 3). F3

Statistical Analysis

All statistical analyses were performed using MedCalc15.6.1 software (MedCalc Software bvba, Ostend, Belgium; https://www.medcalc.org; 2015). Continuous variables were expressed as the mean and standard deviation, and categorical variables were expressed as frequency and percentage. The difference of CT-FFR values between the 2 scanning techniques was compared using paired Wilcoxon signed-rank test. The consistency of CT-FFR values was tested by Pearson correlation value and Bland-Altman. Statistical significance was set at $P < 0.05$.

RESULTS

Patient Population

A total of 146 patients were initially considered for inclusion in the study. Of these, 24 patients were excluded because their CCTA images were not available for CT-FFR computational analysis. Eleven patients were excluded because of severe coronary artery artifacts due to severe calcification, 3 patients had coronary artery malformation, and 10 patients had a history of coronary artery stenting. Finally, a total of 366 coronary arteries from the remaining 122 patients were analyzed. The clinical characteristics of all the patients are shown in Table 1. T1

Coronary Computed Tomography Angiography–Derived Fractional Flow Reserve Analysis

There was no significant difference regarding the lowest CT-FFR values between systole phase and diastole phase across all vessels (Table 2). In addition, there was no significant difference in the lesion CT-FFR value (at 2 cm distal to the stenosis) after coronary artery stenosis between systole phase and diastole phase across all vessels (Table 3). T2 T3

Correlation Analysis

In the analysis of each vessel, the lowest CT-FFR values of systole phase and diastole phase were well correlated (Fig. 4). F4

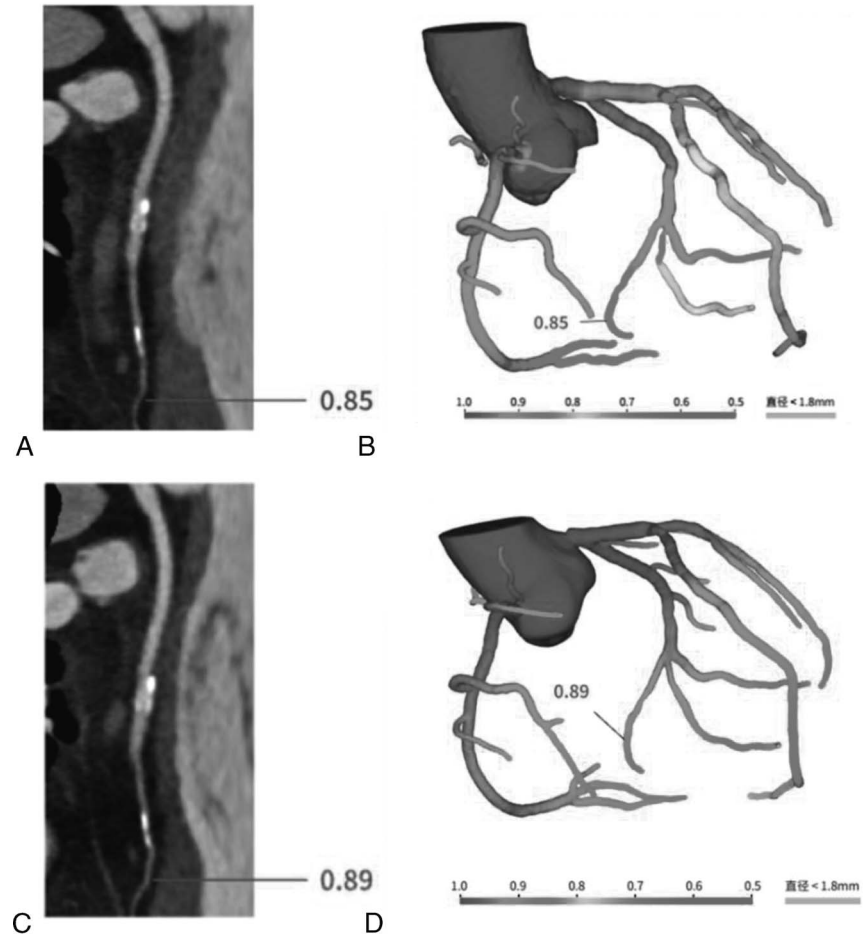

FIGURE 3. An example of the CCTA and the corresponding CT-FFR model, a 65-year-old male patient. A and C, LCX with mild stenosis imaged by CCTA selected 2 optimal phases of systolic phase and diastolic phase for reconstruction. B, The corresponding CT-FFR model of systolic phase for reconstruction. The minimum CT-FFR value (the CT-FFR value at the distal end of each vessel) was shown as 0.85. D, The corresponding CT-FFR model of diastolic phase for reconstruction. The minimum CT-FFR value (the CT-FFR value at the distal end of each vessel) was shown as 0.89. Figure 3 can be viewed in color online at www.jcat.org.

TABLE 1. Patient Characteristics (N = 122)

Age, y	63.1 ± 7.8
Male	87 (71.3)
Body mass index, kg/m^2	24.9 ± 1.6
Cardiac risk factors	
Hypertension	65 (53.3)
Hyperlipidemia	53 (43.4)
Diabetes	39 (32.0)
Smoking	72 (59.0)
Obesity	45 (36.9)
Drinking	30 (24.6)
Symptoms	
Angina pectoris	62 (50.8)
Probable angina pectoris	49 (40.2)
Atypical chest pain	11 (9.0)

Values are expressed as mean ± SD or n (%).

The correlation coefficient of the lowest CT-FFR values for left anterior descending branch (LAD), left circumflex branch (LCx), and right coronary artery (RCA) were 0.63, 0.68, and 0.52, respectively (Fig. 4). The lesion CT-FFR value (at 2 cm distal to the stenosis) after coronary artery stenosis had excellent correlation (Fig. 5). The correlation coefficient of the lesion CT-FFR values for LAD, LCx, and RCA were 0.86, 0.84, 0.76, respectively (Fig. 5).

TABLE 2. The Minimum CT-FFR Value: Systolic Versus Diastolic Scan Acquisition

	Systolic Phase	Diastolic Phase	*P*
LAD	0.780 (0.730–0.810)	0.770 (0.720–0.800)	0.106
LCx	0.875 (0.830–0.910)	0.870 (0.830–0.910)	0.524
RCA	0.890 (0.860–0.920)	0.890 (0.860–0.910)	0.378

Values are expressed as median.

TABLE 3. Lesion CT-FFR Value: Systolic Versus Diastolic Scan Acquisition

	Systolic phase	Diastolic phase	*P*
LAD	0.870 (0.830–0.915)	0.870 (0.850–0.900)	0.513
LCx	0.890 (0.860–0.930)	0.900 (0.870–0.930)	0.914
RCA	0.870 (0.840–0.925)	0.885 (0.855–0.910)	0.981

Values are expressed as median.

Bland-Altman analysis of CT-FFR values—systolic versus diastolic scan acquisition—showed minimal bias (Fig. 6). The results revealed that the deviations between of the lowest CT-FFR value of the LAD, LCx, and RCA, and between the lesion CT-FFR value (at 2 cm distal to the stenosis) after coronary artery stenosis were negligible (Table 4).

DISCUSSION

To the best of our knowledge, this study reports the first retrospective and direct validation of the stability of an artificial intelligence-based deep learning neural network-based CT flow reserve fraction analysis method in systolic and diastolic heart beats. The time consistency of contrast agent turbidity had no effect on CT-FFR measurement of coronary arteries. Our results support the effectiveness of CT-FFR in calculating coronary flow reserve fraction and evaluating coronary artery stenosis regardless of scan acquisition phase.

Coronary artery disease is the leading cause of cardiovascular mortality and morbidity across the globe.[18] Fractional flow reserve is the "criterion standard" to evaluate the physiological function of coronary arteries.[19,20] Fractional flow reserve–guided percutaneous coronary intervention can improve the prognosis of patients.[21–23] However, FFR is an invasive test with high cost and limited clinical application.[24,25]

Based on the training and learning of fluid dynamics simulation data of a large number of coronary artery cases, the software for calculation of coronary blood flow reserve fraction adopts the self-developed deep learning technology for vessel segmentation and reconstruction and calculation of blood flow reserve fraction.[3] In recent years, CT-FFR has developed rapidly. Many studies have reported that CT-FFR has a higher diagnostic accuracy than other noninvasive examination modalities for heart disease, compared with the criterion standard invasive FFR.[2,4,6] Ideally, coronary CTA data collection should be obtained within the cardiac cycle of a single-phase, but because of the heart's beat, inability to control the rapid heart rate, and limiting factors such as scanning equipment,[10] the scan time of diastolic and systolic capture images leads to the existence of different contrast-medium transmission time nonuniformity.[9,11] Hence, we focused on the uniformity of the time problem, as it depends on the CT scan acquisition protocol.

In our study, there was no significant difference in the lowest CT-FFR value between systolic phase and diastolic phase across all vessels. In addition, there was no significant difference in the lesion CT-FFR value after coronary artery stenosis. The CT-FFR value between the 2 reconstruction techniques had excellent correlation and minimal bias in all groups. The lesion CT-FFR value after coronary artery stenosis showed excellent correlation, with a correlation coefficient of LAD, LCx, and RCA were 0.86, 0.84, and 0.76, respectively. The 3 main coronary arteries were not affected by the temporal uniformity of scanning acquisition protocol, and the evaluation of hemodynamics after coronary artery stenosis was highly consistent.

LIMITATIONS

Our study has some limitations. First, this study mainly verified the influence of CT scanning technology on the accuracy of CT-FFR data collection. The same concentration of contrast agent was used in the experiment, without analyzing whether different concentrations would affect the collection of CT-FFR values. Second, 320-slice CT was used to complete coronary CTA scanning in this study, and the effect of 64-slice CT was not verified. Therefore, the results of this study may not be generalizable to other CT scanners. Third, patients with severe coronary artery calcification were excluded in this study, mainly those patients with severe image artifacts caused by severe calcification. Because we did not carry out calcification score quantitative grading, this needs to be further verified in subsequent experiments. Fourth, this study had a lack of validation of CT-FFR results by invasive FFR. Although we focused on

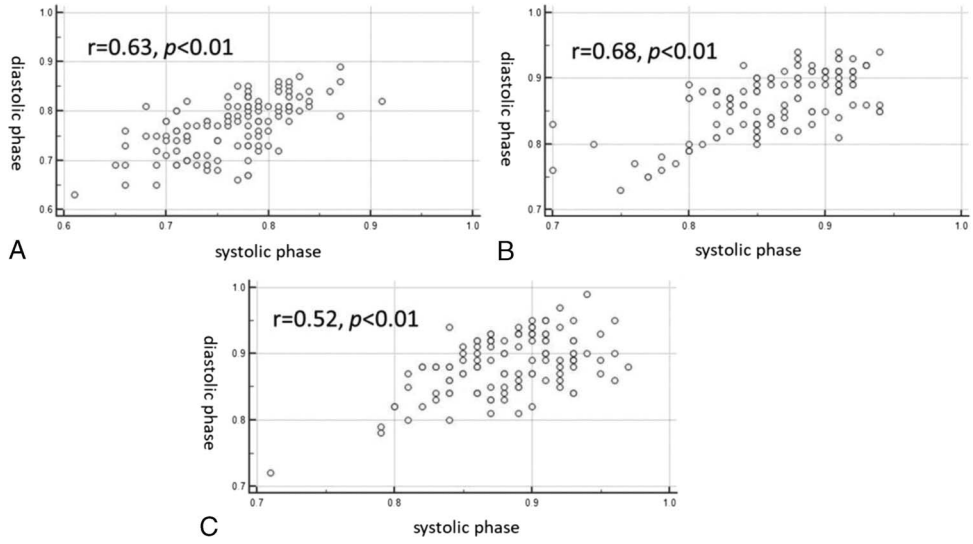

FIGURE 4. The minimum CT-FFR value (the CT-FFR value at the distal end of each vessel): systolic versus diastolic scan acquisition in a single heartbeat. The minimum CT-FFR value showed good correlation. A, LAD, B, LCX, C, RCA. "Figure _ can be viewed online in color at www.jcat.org."

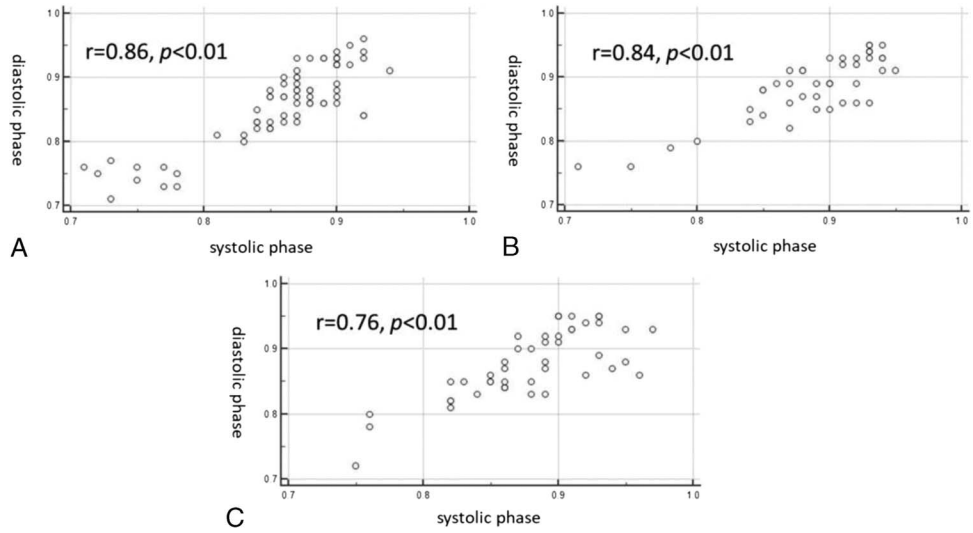

FIGURE 5. The lesion CT-FFR value (at 2 cm distal to the lesion) after coronary artery stenosis: systolic versus diastolic scan acquisition in a single heartbeat. The lesion CT-FFR value showed excellent correlation. A, LAD, B, LCX, C, RCA. "Figure _ can be viewed online in color at www.jcat.org."

comparison of CT-FFR findings between 2 acquisition protocols, the accuracy and validation of CT-FFR by invasive FFR are necessary. Fifth, because the software was stable during the operation results of image processing in the same time phase, we did not perform repeatability verification, nor did we carry out a comparative analysis of the accuracy of CT-FFR value calculated by different artificial intelligence software. It would be interesting to perform repeatability verification and compare different CT-FFR methods as our future study. Besides, as we know, CCTA is now recommended as a noninvasive method to exclude CAD in population with low possibility of CAD. It is reasonable to suspect that far more participants with mild than who with moderate or severe

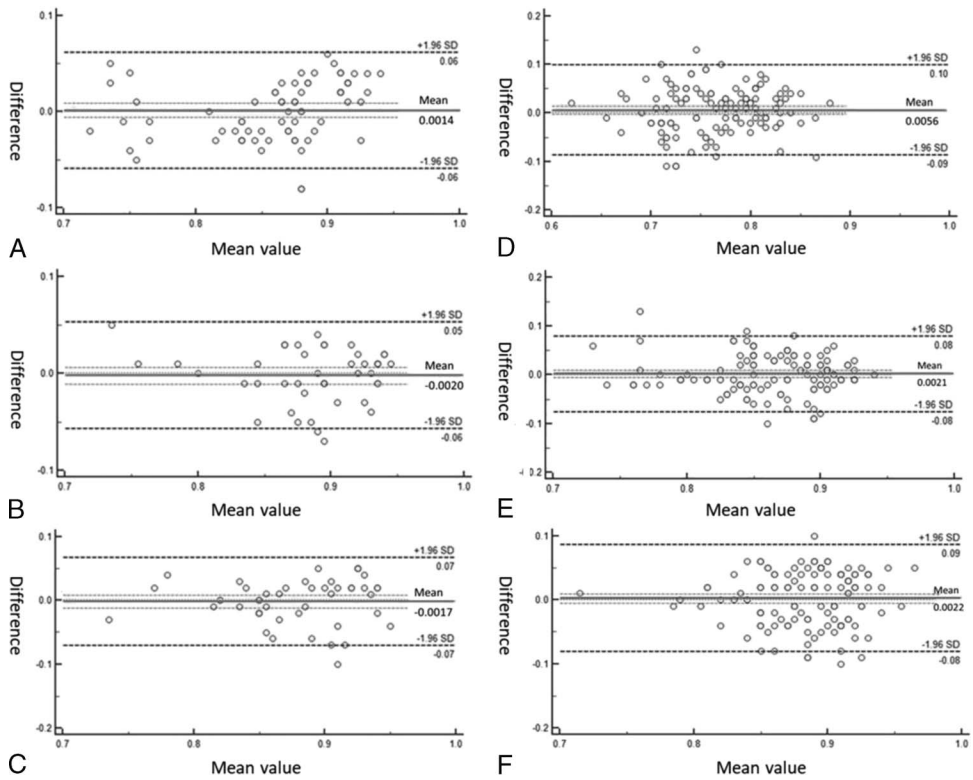

FIGURE 6. Bland-Altman analysis of CT-FFR values: systolic versus diastolic scan acquisition. The CT-FFR value of systolic and diastolic phase images showed minimal bias. The lesion CT-FFR value (at 2 cm distal to the lesion) after coronary artery stenosis for (A) LAD, (B) LCx, and (C) RCA. The minimum CT-FFR value (the CT-FFR value at the distal end of each vessel) for (D) LAD, (E) LCx, (F) RCA. Figure 6 can be viewed in color online at www.jcat.org. "Figure _ can be viewed online in color at www.jcat.org."

TABLE 4. Mean Difference, SD, and Limits of Agreement in Bland-Altman Analysis

	Lesion LAD	Lesion LCx	Lesion RCA	Lowest LAD	Lowest LCx	Lowest RCA
Mean difference	0.0014	−0.0020	−0.0017	0.0056	0.0021	0.0022
SD	0.0308	0.0282	0.0351	0.0474	0.0396	0.0427
Upper limit	0.0617	0.0531	0.0671	0.0986	0.0798	0.0860
Lower limit	−0.0589	−0.0573	−0.0704	−0.0874	−0.0756	−0.0815

Values are derived from Bland-Altman analysis. Lesion means the lesion CT-FFR value (at 2 cm distal to the stenosis); lowest means the lowest CT-FFR value (the CT-FFR value at the distal end of each vessel).

coronary stenosis were included in this study, which could overestimate the ability of CT-FFR based on deep learning. Lastly, patients with stents were excluded from the experiment, mainly because of the small number of patients, and the accuracy of CT-FFR for patients with stents remains to be verified in future studies.

CONCLUSIONS

Coronary computed tomography angiography–derived fractional flow reserve based on artificial intelligence deep learning neural network has stable performance, is not affected by the acquisition phase technology of 320-slice CT scan, and has high consistency with the evaluation of hemodynamics after coronary artery stenosis.

REFERENCES

1. Taylor CA, Fonte TA, Min JK. Computational fluid dynamics applied to cardiac computed tomography for noninvasive quantification of fractional flow reserve: scientific basis. *J Am Coll Cardiol*. 2013;61:2233–2241.
2. Driessen RS, Danad I, Stuijfzand WJ, et al. Comparison of coronary computed tomography angiography, fractional flow reserve, and perfusion imaging for ischemia diagnosis. *J Am Coll Cardiol*. 2019;73:161–173.
3. Tang CX, Liu CY, Lu MJ, et al. CT FFR for ischemia-specific CAD with a new computational fluid dynamics algorithm: a Chinese multicenter study. *JACC Cardiovasc Imaging*. 2020;13:980–990.
4. Tanaka K, Bezerra HG, Gaur S, et al. Comparison between non-invasive (coronary computed tomography angiography derived) and invasive-fractional flow reserve in patients with serial stenoses within one coronary artery: a NXT trial substudy. *Ann Biomed Eng*. 2016;44:580–589.
5. Tesche C, De Cecco CN, Albrecht MH, et al. Coronary CT angiography–derived fractional flow reserve. *Radiology*. 2017;285:17–33.
6. Patel MR, Norgaard BL, Fairbairn TA, et al. 1-Year impact on medical practice and clinical outcomes of FFRCT: the ADVANCE Registry. *JACC Cardiovasc Imaging*. 2020;13:97–105.
7. Tang CX, Wang YN, Zhou F, et al. Diagnostic performance of fractional flow reserve derived from coronary CT angiography for detection of lesion-specific ischemia: a multi-center study and meta-analysis. *Eur J Radiol*. 2019;116:90–97.
8. Ohnesorge BM, Hofmann LK, Flohr TG, et al. CT for imaging coronary artery disease: defining the paradigm for its application. *Int J Cardiovasc Imaging*. 2005;21:85–104.
9. Stuijfzand WJ, Danad I, Raijmakers PG, et al. Additional value of transluminal attenuation gradient in CT angiography to predict hemodynamic significance of coronary artery stenosis. *JACC Cardiovasc Imaging*. 2014;7:374–386.
10. Hsiao EM, Rybicki FJ, Steigner M. CT coronary angiography: 256-slice and 320-detector row scanners. *Curr Cardiol Rep*. 2010;12:68–75.
11. Celeng C, Leiner T, Maurovich-Horvat P, et al. Anatomical and functional computed tomography for diagnosing hemodynamically significant coronary artery disease: a meta-analysis. *JACC Cardiovasc Imaging*. 2019;12:1316–1325.
12. Leipsic J, Abbara S, Achenbach S, et al. SCCT guidelines for the interpretation and reporting of coronary CT angiography: a report of the Society of Cardiovascular Computed Tomography Guidelines Committee. *J Cardiovasc Comput Tomogr*. 2014;8:342–358.
13. Cury RC, Abbara S, Achenbach S, et al. Coronary Artery Disease–Reporting and Data System (CAD-RADS): an expert consensus document of SCCT, ACR and NASCI: endorsed by the ACC. *JACC Cardiovasc Imaging*. 2016;9:1099–1113.
14. Wang ZQ, Zhou YJ, Zhao YX, et al. Diagnostic accuracy of a deep learning approach to calculate FFR from coronary CT angiography. *J Geriatr Cardiol*. 2019;16:42–48. AQ5
15. Li Y, Qiu H, Hou Z, et al. Additional value of deep learning computed tomographic angiography-based fractional flow reserve in detecting coronary stenosis and predicting outcomes. *Acta Radiol*. 2022;63:133–140.
16. Liu X, Mo X, Zhang H, et al. A 2-year investigation of the impact of the computed tomography-derived fractional flow reserve calculated using a deep learning algorithm on routine decision-making for coronary artery disease management. *Eur Radiol*. 2021;31:7039–7046.
17. Gao Z, Wang X, Sun S, et al. Learning physical properties in complex visual scenes: an intelligent machine for perceiving blood flow dynamics from static CT angiography imaging. *Neural Netw*. 2020;123:82–93.
18. Lucas FL, DeLorenzo MA, Siewers AE, et al. Temporal trends in the utilization of diagnostic testing and treatments for cardiovascular disease in the United States, 1993–2001. *Circulation*. 2006;113:374–379.
19. Danad I, Szymonifka J, Twisk JWR, et al. Diagnostic performance of cardiac imaging methods to diagnose ischaemia-causing coronary artery disease when directly compared with fractional flow reserve as a reference standard: a meta-analysis. *Eur Heart J*. 2017;38:991–998.
20. Gotberg M, Christiansen EH, Gudmundsdottir IJ, et al. Instantaneous wave-free ratio versus fractional flow reserve to guide PCI. *N Engl J Med*. 2017;376:1813–1823.
21. Fearon WF, Nishi T, De Bruyne B, et al. Clinical outcomes and cost-effectiveness of fractional flow reserve–guided percutaneous coronary intervention in patients with stable coronary artery disease: three-year follow-up of the FAME 2 trial (fractional flow reserve versus angiography for multivessel evaluation). *Circulation*. 2018;137:480–487.
22. De Bruyne B, Pijls NH, Kalesan B, et al. Fractional flow reserve–guided PCI versus medical therapy in stable coronary disease. *N Engl J Med*. 2012;367:991–1001.
23. Tonino PA, Fearon WF, De Bruyne B, et al. Angiographic versus functional severity of coronary artery stenoses in the FAME study fractional flow reserve versus angiography in multivessel evaluation. *J Am Coll Cardiol*. 2010;55:2816–2821.
24. De Bruyne B, Fearon WF, Pijls NH, et al. Fractional flow reserve–guided PCI for stable coronary artery disease. *N Engl J Med*. 2014;371:1208–1217.
25. Johnson NP, Jeremias A, Zimmermann FM, et al. Continuum of vasodilator stress from rest to contrast medium to adenosine hyperemia for fractional flow reserve assessment. *JACC Cardiovasc Interv*. 2016;9:757–767.

AUTHOR QUERIES

AUTHOR PLEASE ANSWER ALL QUERIES

AQ1 = Please indicate highest academic degree(s) (eg, MD, PhD) of each author.

AQ2 = Please check if the captured affiliations are accurate.

AQ3 = Address information of the corresponding author must be composed of street address, abbreviated state, zip code, and country if not USA. Please supply missing data.

AQ4 = Please check if this statement has been captured correctly.

AQ5 = Ref. 18 was a duplicate and was thus removed from the Reference list. Please check if appropriate.

END OF AUTHOR QUERIES